ACS OMEGA

http://pubs.acs.org/journal/acsodf

Article

Efficient Water Collection from Biodesigned and Natural Inclined Surfaces: Influence of Inclination Angle on Atmospheric Water Collection

Edward Hingha Foday, Jr,* Taiwo Sesay, Yagbasuah Maada Baion, Emmanuel Bartholomew Koroma, Alpha Yayah Jalloh, Kejan Kokofele, and Florence Wuyah Baion

Cite This: *ACS Omega* 2022, 7, 43574−43581

Read Online

ACCESS | Metrics & More | Article Recommendations

ABSTRACT: Water is one of the most important and crucial indicators of sustainable development goals (SDGs) for humans and other living organisms. Water demand has outstripped supply, resulting in shortage on a worldwide scale, particularly in arid regions. This water scarcity has impeded agricultural productivity and other developmental projects with the ongoing global warming and other anthropogenic activities making it more complicated. To address the worldwide water crisis, it is worthwhile to convert atmospheric air to drinking water. Sequel to that, a hydrophobic surface was designed using facile lithography to compare its water harvesting efficiency with a hydrophilic surface at different orientation angles. For the research, the hydrophobic designed surface is called biodesigned material, while the hydrophilic natural surface is a *Mangifera indica* leaf (MIL). It is against this background that we seek to investigate the most suitable orientation angle good for efficient water harvesting. To that end, a 60° inclination angle is the most efficacious orientation for water collection as it outperformed the 30 and 45° orientation angles. To minimize re-evaporation, absorption, suction, and other environmental challenges that impede efficient collection, atmospheric moisture should be collected immediately from functional surfaces.

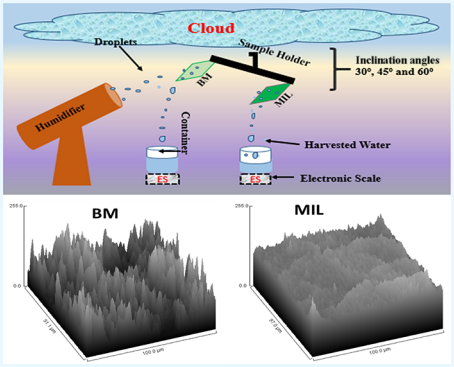

1. INTRODUCTION

All floras and faunas including mankind need water for survival as it is one of the most essential and indispensable indicators significant for achieving sustainable development goals (SDGs).[1,2] Therefore, ensuring adequate availability of water is imperative for human beings and the planet as a whole. Because of the ubiquity of water in the atmosphere, particularly on the planet Earth, which is often called the "Blue Planet", water shortage is at an alarming level. Universally, about 2 billion people lack safe drinking water and about two-fifths suffer from the consequences of unacceptable sanitary conditions.[3,4] Atmospheric water represents an invaluable untapped source of fresh water, especially in desert and arid regions. When the water demand exceeds the available water, the scarcity level increases. For this research, we describe such a mismatch between water availability and demand as water scarcity. For example, the Saharan and Arabian Deserts suffer from water scarcity considering their high population that does not match the available water.[5] This water scarcity has impeded agricultural productivity and other developmental projects. However, with the exception of atmospheric moisture, other water sources are diminishing daily by both anthropogenic activities and rapid population growth alongside poor environmental management.[6,7] As a result of these environmental ills, water scarcity is foretold to be one of the severest issues in contemporary times. It is predicted that many more places around the world will experience water scarcity in the future, thereby resulting in poor sanitation.[6,8] To that end, the already available over-stressed water resources are further complicated by the ongoing climate change which urgently calls for holistic approaches to tackle this global water conflict.[9,10] Apart from the desalination of seawater and the treatment of wastewater as a solution, atmospheric water collection has attracted researchers as a potential remedy to the global water crisis.[11,12] It is believed that the atmosphere holds about 12,900 billion tons of fresh water, which are continuously replenished by global water circulation.[13,14] In recent years, the atmospheric water behavior on flora and fauna surfaces has inspired engineers to fabricate synthetic surfaces from polymeric materials.[15,16] Similarly, sorption-based atmos-

Received: July 9, 2022
Accepted: November 10, 2022
Published: November 22, 2022

pheric water harvesting (SAWH) has taken the center stage in ameliorating the water crisis. This method, which relies primarily on electric or thermal energy, employs sorbents because of their great affinity to absorb water from the air across a wide range of RH (10−100% RH).[17,18] The performance of SAWH systems is strongly dependent on the water sorption capacity of sorbents, giving them a significant advantage over conventional methods.[19]

Desert plants and animals species have offered ingenious ways of collecting water from the atmosphere;[20] examples include the Hipster herb that possesses ultra-hydrophobic hair on its leaves,[21] *Cotulla fallax* with uncanny wetting properties,[22] green tree frogs,[26] Namib grass,[24] and Australian desert lizards.[25] The water collection mechanism of natural animals and plants such as cactus, spiders, desert beetles, butterflies, shorebirds, wheat awns, green bristle grass, *Cotulla fallax* plant, Namib grass, green tree frogs, and Australian desert lizards was detailed by Zhu et al.[23] For example, the Namib beetle can absorb humidity from the environment as a result of the wetting property of its body surface. The backside surface of the beetle consists of both hydrophilic and hydrophobic regions, thus playing a dual role in droplet formation and absorption. Water is collected from the smooth and rough surface on the backside of the beetle before droplets are inclined to the upper wing, thereby gathering and guiding the droplets to the mouth of the beetle.[27−29] For biomimetic water-collecting materials, Guo and Zhu[30] used TiO_2 and Cu to design a surface with hydrophilic and hydrophobic regions, respectively, thus exhibiting a water collection rate (WCR) of 1309.9 mgh^{-1} cm^{-2}. Similarly, White et al.[31] tested other samples (e.g. PTFE, Al, Ti, and SS-CNT) to better understand the wetting properties with respect to the pattern structure surfaces, and they found that there were slight differences in the coalescence and motion of the droplets on the differently patterned surfaces. For effective water collection, droplets' interaction with the substrate before collection is unavoidable, and dripping off from the substrate for efficient water harvesting is significant in our lives and other fields such as microfluidics, spraying, and the survival of natural species. Plenty of these natural species use their surface structures to transport and drain water. Surface features such as bumps, apex, curvature, spines, and other features have all been researched and proven useful in efficient water collection.[32,33] Even though these delicate features have performed well, they have disregarded the droplet roll-off time and inclination angle in determining water collection efficiency. The droplet behaviors on these functional surfaces are often determined by these surface features, thus playing the key role in reducing the capillary force, while inclined surfaces enhance the high frequency of droplet roll-off.

The angle of inclination of the functional surface alongside contact angle hysteresis plays a key role in droplet roll-off, thus paving the way for gravity and low water retention. Sessile droplets on both hydrophobic and hydrophilic surfaces were examined for internal fluidity, and it was found that the droplet contains two counter-rotating circulation cells.[34] Marangoni and buoyancy forces were said to have an impact on the droplet behavior for the hydrophilic surface, whereas thermal capillary and buoyant forces have an impact on the droplet behavior for the hydrophobic surface. Even at high inclination angles, droplets stick to hydrophobic surfaces with high-contact angle hysteresis due to the considerable adhesive force that remains.[35] Droplet attachment is facilitated by force balancing along the inclined surface, and in this case, the rotating and sliding modes of droplet movement dictate the droplet's dynamic motion. Annapragada et al.[36] also studied the dynamics of the droplet on an inclined surface by adopting a pseudo-Lagrangian methodology, which was based on the "volume of fluid" minus "continuous surface force" (VOF − CSF) model. This model represents the migration of droplets down an inclined surface. Thampi et al.[37] studied the rolling and sliding behavior of droplets on an inclined surface. They found that the viscosity variance between the droplet and ambient fluid became large as the rolling droplet achieved a circle shape.

When a droplet is deposited on an inclined surface, shear stress develops at the contact zone interface, resulting in the formation of a flow field. As a result of this process, frictional force is created at the solid−droplet contact. Droplet movement on an inclined surface is influenced by droplet bulging/puddling due to a gravitational effect when the gravitational force exceeds the adhesion and frictional forces.[38] Adhesion force is proportional to $\pi r\sigma(\cos\theta_R - \cos\theta_A)$, where r, θ_R, and θ_A denote the radius of the contact zone, receding angle (upward hill), and advancing angle (downward hill), respectively, while σ defines the droplet surface tension. When fluid viscosity (μ) and the rate of fluid strain to the contact surface is dV/dn, the shear force is defined as $\pi r^2\mu\, dV/dn$. This shear force exceeds gravitational force and is consequently connected with $mg \sin\delta$ (where m, g, and δ are the mass of a droplet, gravity, and inclined surface).[39]

Although natural and biomimetic surfaces have proven successful in harvesting atmospheric water, the transportation of liquid droplets is the key to the roll-off of captured droplets from the surfaces. In this work, we seek to carefully design a *Mangifera indica* leaf (MIL) with PDMS and mimic its surface with calcium chloride anhydrous ($CaCl_2$) nanoparticles to achieve a uniform wettable surface similar to the MIL surface. Similarly, we will compare the efficiency of water collection across the hydrophobic biodesigned and hydrophilic natural surfaces at various inclination angles. In addition, the variation of surface wettability between the functional surfaces will be investigated. To this intent, the actual roll-off time at different inclination angles will be monitored alongside the droplet dynamics on the functional surfaces. The findings of this study will shed light on the critical effect of an inclination angle on efficient water harvesting and thus promote atmospheric water collection as an alternative to address the global water crisis.

2. EXPERIMENTAL SECTION

2.1. Materials. PDMS kits, ethanol, and calcium chloride anhydrous ($CaCl_2$) nanoparticles were supplied by Biochemical Co., Ltd., Shanghai, China, while a fresh *M. Indica* leaf was obtained from Yunnan Provinces, China. Sandpaper, which was used to prepare the surface roughness was obtained from statske Co., Ltd., China. A humidifier, hydrometer, and anemometer were purchased from YADU Science and Technology Co., Ltd., Beijing. Fiji(ImageJ) and origin Pro were used for data analysis, while transparent acrylic was set up as a micro-weather.

2.2. Surface Fabrication. The experimental surface was replicated using PDMS and calcium chloride anhydrous ($CaCl_2$) nanoparticles. Inspired by *M. indica*, $CaCl_2$ nanoparticles were used to mimic the surface wettability of the designed surface. The surface was dressed with $CaCl_2$ nanoparticles using a facile lithography method (Figure 1). A

https://doi.org/10.1021/acsomega.2c04344
ACS Omega 2022, 7, 43574−43581

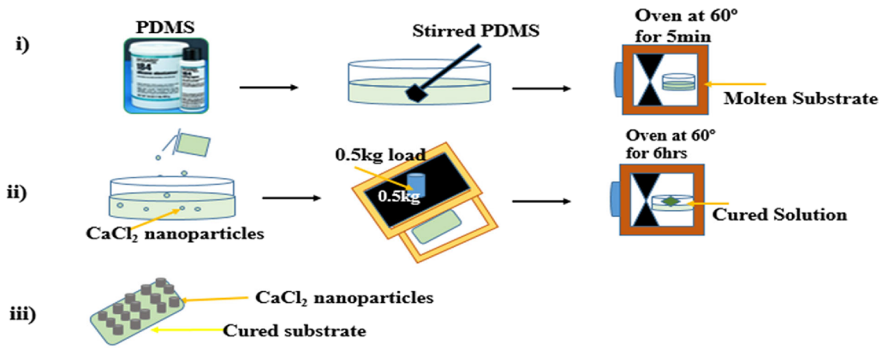

Figure 1. Biodesigned natural MIL using the soft lithography process. (i) First stage: PDMS molten substrate preparation stage; (ii) second stage: application of $CaCl_2$ nanoparticles on the molten substrate; and (iii) final stage: finished product (biodesigned substrate).

ratio of 20:2 of elastomer (Sylgard 184A/B, Dow Corning) mass was prepared and stirred in a glass cup using a silver rod. The air bubbles were removed using a vacuum desiccator before being set in an oven for 5 min at 60 °C. The ($CaCl_2$) nanoparticles were gently spread over the semi-cured molten substrate. The semi-cured molten substrate was covered with light transparent glass as a 0.5 kg weight solid object was placed on the top to ensure that ($CaCl_2$) nanoparticles are neatly attached to the surface of the substrate. Finally, the semi-molten substrate was again placed in an oven for 6 h to achieve full cure. For this paper, the end-product of this fabrication sample has been called biodesigned material (BM), while a natural *M. indica* leaf (MIL) was used without further modification. Sandpaper was used to reduce highly protruded grooves on the BM surface to maintain surface uniformity, while ethanol was used to clean the specimens.

2.3. Water Collection. The water collection experiment was performed using fresh MIL and PDMS dressed with ($CaCl_2$) nanoparticles. The samples were carefully fixed onto a sample holder at inclination angles of 30, 45, and 60° from the horizontal plane, as shown in Figure 2. The atmospheric

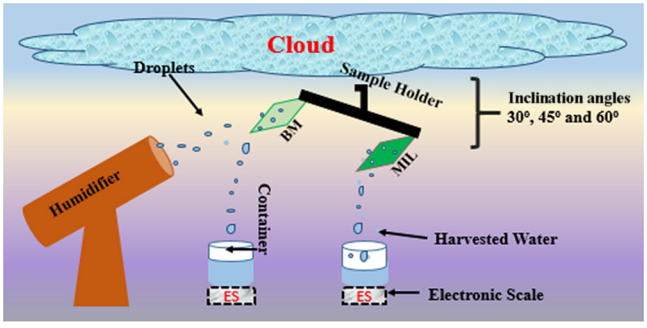

Figure 2. Schematic illustration of the water collection experimental setup.

moisture was generated by a D20 humidifier under a humidity and temperature of 80% and 21 ± 2 °C respectively. An anemometer was utilized to measure the atmospheric water velocity (2.5 ms^{-1}) as the samples were perpendicularly placed 5 cm away from the sample holder. The BM and MIL surfaces were of uniform sizes with an area of about 3 × 2cm. The entire process was recorded with an optical microscope (VHX-900) and digital camera (Nikon-D90), while the total weight of water was measured by an electronic scale (JY501). The weight was measured every 30 min cycle for 90 min as the collection time was the key in determining the surface with the most efficient water collection with respect to their respective inclination angles. Fiji (ImageJ) and origin Pro were used for data analysis, while transparent acrylic was set up as a micro-weather.

2.4. Characterization. Surface morphology was investigated by a scanning electron microscope (SEM, HITACHI-S-4800), while the mechanical properties of the functional surface were investigated by a Universal Testing Machine (WDW-20; Shijin, China). Surface wettability was investigated using an OCA (JC-200D-1), while the droplet behavior on the functional surfaces was studied using a VHX-900F.

3. RESULTS AND DISCUSSION

3.1. Surface Design Rationale and Wettability. PDMS and $CaCl_2$ nanoparticles were used to biodesign the surface of MIL for effective water collection. To that end, it is important to design a surface that attracts nucleation without compromising the movement of droplets similar to the MIL. The surface smoothness alongside the flatness of the fabricated PDMS substrate leads to a relatively low droplet nucleation event. Sequel to that, we designed the surface with $CaCl_2$ nanoparticles to mimic the surface of MIL, as shown in Figure 1. The biodesigned surface has microgrooves with a dimensional width of 5−7 mm, height of 4−6 mm, and spacing of 2−5 mm alongside the natural material with a similar surface area that was placed at different orientations during the experiment. The surface roughness (R_a) of MIL and BM surfaces was investigated with suitable image software (Fiji/ImageJ). The BM has a roughness value of 19.5 μm, while MIL gives a value of 27.4 μm, thus defining MIL to have a rougher surface than the BM (Figure 3a). However, the designed microgroove on the BM surface helps retain tiny droplets in between the grooves similar to the droplet behavior visualized on the hydrophilic surface (MIL). The surface wettability of both MIL and BM (chemically homogeneous solid surface) was investigated, which reflects Young's equation.[40] We determined the static, receding, and advancing angles using a goniometer (JC 200D-1) with a 5 μL sessile droplet. Comparing the BM surface with MIL, the BM surface exhibits a higher contact angle, which depicts hydrophobic characteristics, while the MIL surface exhibits low contact angle (CA), depicting hydrophilic characteristics, as shown in Figure 3b. Similarly, a smaller receding, advancing, and CA hysteresis was seen for MIL when compared to the BM surface, as shown in Table 1. This was as a result of the pinning effects of liquid droplets on the microgroove surface of MIL, which possesses hydrophilic features compared to the BM surface.

https://doi.org/10.1021/acsomega.2c04344
ACS Omega 2022, 7, 43574−43581

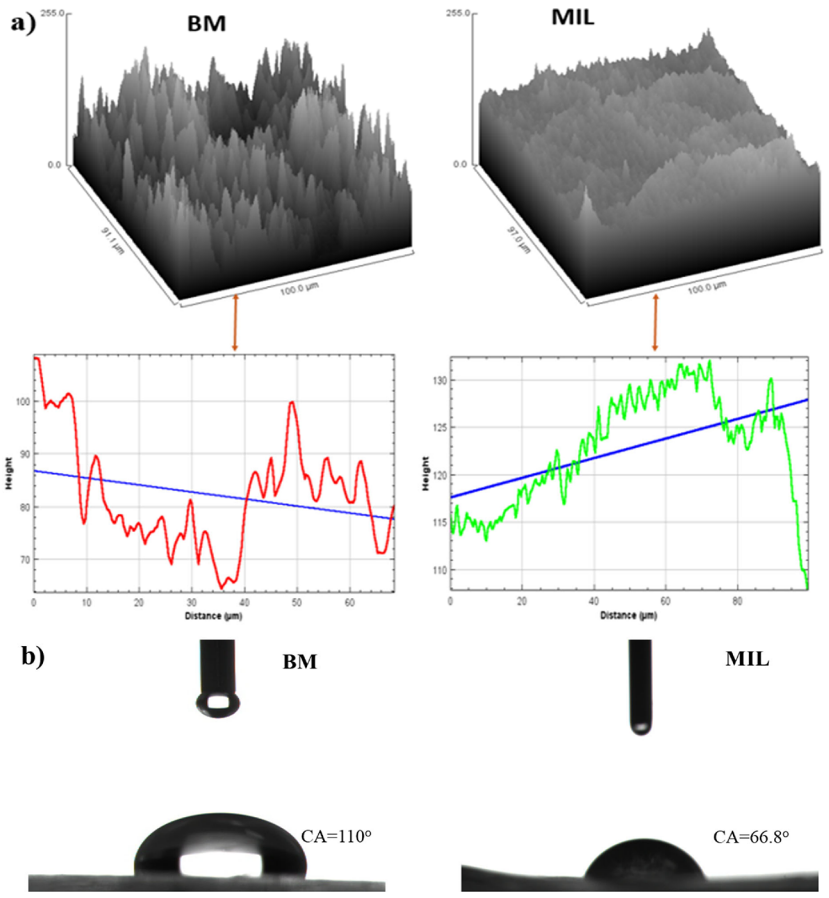

Figure 3. Surface morphology. (a) Surface roughness of both the biodesigned surface (BM) and *M. indica* leaf (MIL). (b) Contact angle (CA) of functional surfaces with a (5 μL) sessile droplet on both BM and MIL surfaces.

Table 1. Surface Wettability

materials	surface feature	contact angle (θ)	advancing contact angle (θ_A)	receding contact angle (θ_R)	contact angle hysteresis (CAH)
BM	hydrophobic	110°	117.9°	102.2°	15.7°
MIL	hydrophilic	66.8°	72.2°	61.7°	10.5°

3.2. Droplet Behavior on Functional Surfaces. Droplet behaviors were investigated microscopically (VHF-900) by comparing the droplets' movement on the functional surfaces (MIL and BM) at different inclined orientations (30, 45, and 60°). However, the hydrophilic MIL surface as compared to the designed hydrophobic BM surface provoked more surface nucleation, thus facilitating the droplet merging and mobility process at the aforementioned inclination angles. We further compared the coalescence behavior of droplets on both BM and MIL surfaces, and it was seen that the tiny droplets on the functional surfaces were interconnected with fast dissipation time for MIL than for BM (Figure 4). This was probably because of external environmental factors such as ambient air, suction, and absorption. At the respective inclination angles (30, 45, and 60°), the tiny droplets on the BM surface runoff to the point of collection within 3.0, 1.45, and 1.20 s, respectively, while it took 3.10, 2.0, and 1.25 s on the MIL surface, respectively. One novel phenomenon observed on the BM surface was that the large droplets seated on the microgroove (protruded microstructure, as shown in Figure 4ai) were quick to merge with adjacent droplets, forming liquid columns. This process accelerates the growth and movement of droplets for collection with the help of gravity. The generated moisture sits on the microgroove instead of permeating into the already-designed microgroove. This "sit-on" of droplets on microgrooves is exposed to ambient air and thermodynamics, thereby undermining surface adhesion and efficient collection.

As shown in Figure 4bi, the generated droplets on the MIL surface were sucked or absorbed into the microgroove when compared to BM. The suction behavior of tiny droplets set the stage for a new circle, thereby impeding the formation of large droplets. In our previous work,[41] it was found that it took a total of 6.47 s for a water film to be formed on the MIL surface when compared to the BM surface with 5.90 s. Due to the natural composition of the MIL surface, a liquid bridge was achieved with the continued generation of moisture, thereby eventually covering the microgrooves for collection. Some novel and intriguing departure behaviors of droplets on the functional surfaces were observed and compared during the collection at respective orientation angles (30, 45, and 60°). As seen in Figure 4aii, the BM surface displays a large droplet roll-off at the orientation angles with no unique pathway for droplet mobility. The droplet shedding was random with no specific departure point for collection (assigned with red arrows) as compared to MIL with a unique pathway for droplet mobility. It was observed that large droplets ignite high departure frequency for efficient collection, making it have a comparative advantage over MIL. Another interesting phenomenon observed was that large droplets sitting on the

https://doi.org/10.1021/acsomega.2c04344
ACS Omega 2022, 7, 43574−43581

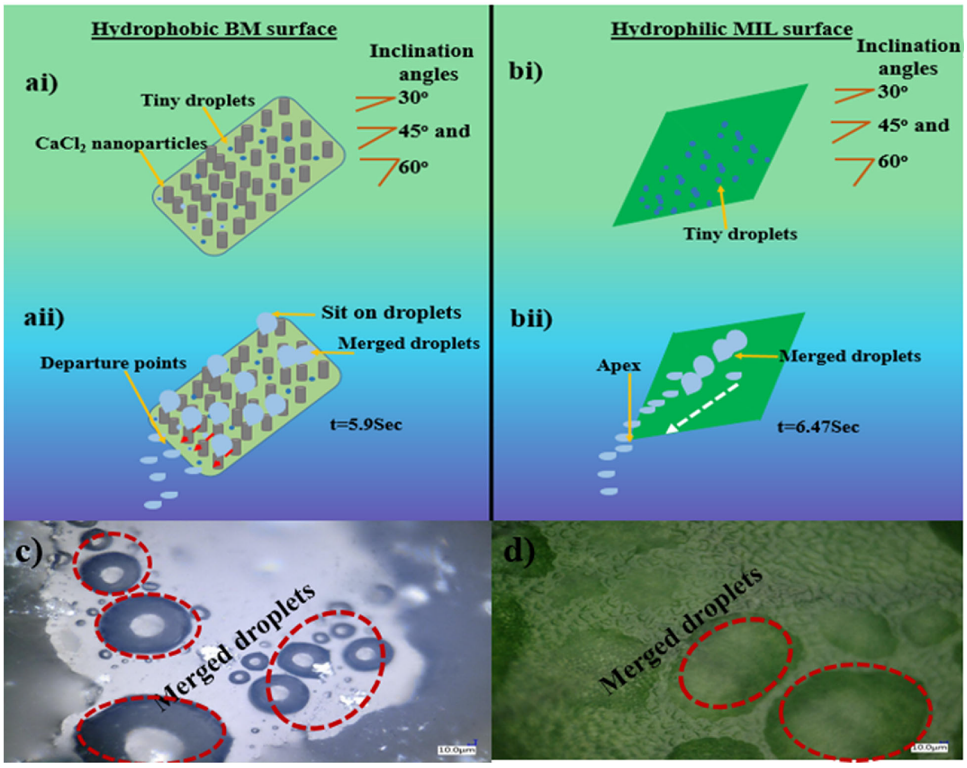

Figure 4. (a) Schematic illustration of the atmospheric water collection on various wettable surfaces (BM and MIL). Microscopy images of the droplet with respect to droplet runoff duration on (b) BM and (c) MIL.

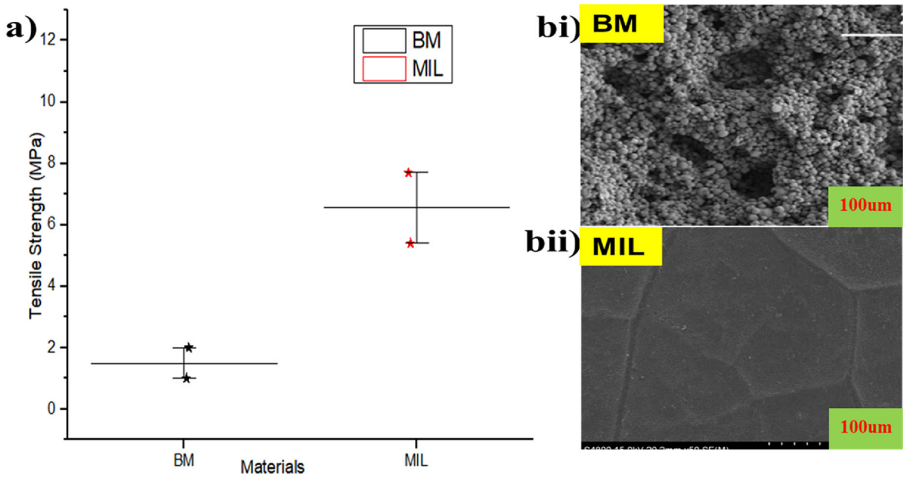

Figure 5. (a) Mechanical properties of the harvesting samples (BM and MIL). (b) SEM images of BM and MIL surfaces.

microgrooves were swept off by the generated falling droplets while a few tiny droplets remained in between the protruded microgrooves of the BM.

Similarly, on the surface of MIL (Figure 4bii), tiny droplets accumulate over time and eventually cover the microgroove to form a water film on the surface for collection at a constant generation of moisture. During the departure process of the water film, pocket droplets are swept flowing over the microgrooves, leading to air in the plughole, a similar scenario reported by Muth and Shank.[42] As the water film grows with respect to the surface area, it overcomes surface adhesion as it reaches the apex for departure. The droplet shedding has a unique pathway (assigned with white arrows) with a specific departure point called the apex. In comparison, droplets interact with fewer surface area on the BM surface as a result of droplet "sit-on" on the microgrooves (Figure 4c), while a large surface area interaction with droplets occurred on the MIL surface based on absorption or suction (Figure 4d). This absorption scenario has resulted in the slow runoff of droplets on the MIL surface when compared to the BM surface.

3.3. Mechanical and Physical Characterization of Substrates. The mechanical properties of the harvesting samples (BM and MIL) were investigated without further modification to ascertain the tensile strength. Before testing, the samples were cut into pieces of uniform shapes and sizes, namely, triangular shapes. The tensile force was exerted on the samples along the direction of the vein, and a pair of rubber pads was fixed on the clamps of the universal testing machine

https://doi.org/10.1021/acsomega.2c04344
ACS Omega 2022, 7, 43574−43581

to prevent the samples from damaging by the clamps. The test of each species was repeated 10 times, and the mean values were calculated and recorded. From Figure 5a, the tensile strengths of BM and MIL were analyzed. The BM provides a higher tensile strength of 7.71 ± 1.21 MPa. One fascinating fact that came out from the mechanical property investigation was the high tensile strength of the BM compared to MIL, which is in total disagreement with the one proposed by Tang et al.,[43] which says that succulent or fresh leaves tend to have a higher tensile strength than biofabricated materials. The MIL has a tensile strength of 5.4 ± 1.23 MPa, which shows lesser tensile strength than BM.

The surface morphology of the water collection substrates was investigated using SEM, as shown in (Figure 5bi,ii). These images displayed the hierarchical microstructure of the surfaces (BM and MIL). Figure 5bi shows the BM surface with protruded structures with well-defined clustered particles. From a magnified observation point, the surface is well covered with ($CaCl_2$) nanoparticles on the surface of the BM with a diameter ranging between 5 and 10 μm. Figure 5bii displays a ridge valley-like surface, which aided the pinning of droplets. The detailed surface morphology of MIL is given in one of our previous papers.[41] Under constant moisture generation conditions, the microgrooves will be filled first before extruding to connect other droplets for collection. At this point, the force of gravity overcomes the retention force at the respective orientation angles (30, 45, and 60°). From the SEM investigation, it can be seen that the BM surface achieved a good degree of mimicking.

3.4. Atmospheric Collection Process. To understand the different performances of each surface in water harvesting, we measured and compared the water collection processes of the functional surfaces. To that end, we horizontally placed the samples at the respective orientation angle for 30 min for each inclination angle (30, 45, and 60°). From the previous literature,[41] the atmospheric water collection process consists of three stages: droplet capturing on the surface, droplet coalescence, and transportation to its terminal point of collection. For this work, we assumed that there is enough supply of moisture on the surface for 90 min with a 30 min cycle time for each orientation angle. During atmospheric water harvesting, numerous generated tiny droplets are sprayed toward the surface and are captured when in direct collision with the functional surface. Due to the small inertia of the colliding droplet as well as adhesion between the incoming droplet and the surface, most of the incoming droplets will be captured onto the surface irrespective of the surface wettability. Based on the aforementioned reason, one can conclude that water transportation at the appropriate inclination angle is a significant factor for efficient water harvesting from a solid surface.

On the hydrophobic BM surface, tiny droplets agglomerated into reasonable droplets as they retained on the wettable surface. Since there was a surface energy gradient and gravity action, tiny droplets on the hydrophobic BM surface were propelled to the departure point, while the large droplets sitting on the microgroove pillars easily roll-off. Similarly, the MIL surface generated a Laplace pressure gradient, which further enhanced the directional movement of water droplets. To validate this assertion, we quantify the water collection efficiency of each surface based on the amount of water collected at different orientation angles (30, 45, and 60°). Figure 6 quantitatively describes the differences in water

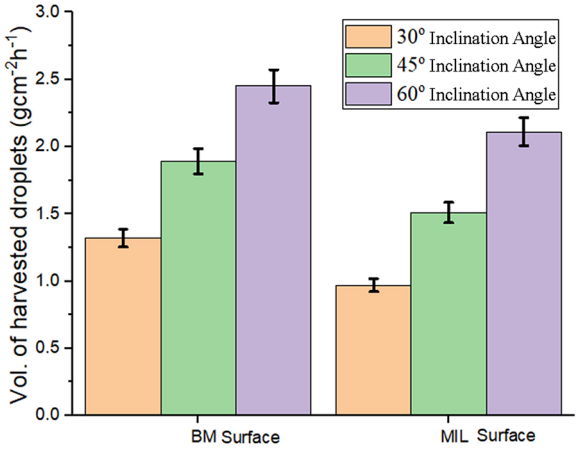

Figure 6. Quantity of harvested water at different inclination angles (30, 45, and 60°). Droplets were harvested from exposed surfaces (BM and MIL) for 90 min with 30 min intervals for each cycle.

collection efficiency of the surfaces with various wettability surfaces. The hydrophobic BM surface harvested more water than the hydrophilic MIL surface as this surface hindered the droplet roll-off due to surface tension. On the hydrophilic MIL surface, the tiny droplets first fill the microgrooves either by absorption or suction before the water film is formed to be moved over the microgrooves under the action of gravity and Laplace pressure, leading to the unidirectional transport process of droplets. It was found that the hydrophilic MIL surface captured more water than the hydrophobic BM surface because the water drops adhered tightly to the hydrophilic surface due to the greater surface tension than the BM hydrophobic surface.

In addition, we compared the water collection efficiency of the functional surfaces by fixing the samples onto the holder at different inclination angles of 30, 45, and 60°. The water collection efficiency was in accordance with the setup shown in Figure 2. These samples were exposed to a moisture flow under a temperature and velocity of 20 ± 1.0 °C and 2.7 ms^{-1}, respectively. From Figure 6, the 60° inclination angle of both surfaces (BM and MIL) displayed the highest water collection efficiency than 30 and 45°. This is as a result of the maximum contact area interacting with the generated moisture from the humidifier. The contact area of the functional samples was calculated using suitable image software (Fiji/ImageJ). The maximum water efficiency of the 60° inclination angle for both BM and MIL surfaces ranges from 30 to 36% and is 20−25% higher than the 30° and 45° inclination angle exposure, respectively. As we altered the inclination angles to 30° and 45°, lower water collection efficiency was achieved when compared to the 60° orientation angle. During the 90 min moisture generation, the BM surface collected a total of 5.66 gcm^{-2} h^{-1} water, while the MIL surface collected a total of 4.59 gcm^{-2} h^{-1}. The overall water collection process occurred at a steady rate with the 60° inclination angle, showing a very good water collection efficiency over the other orientation angles (30 and 45°). Similarly, the hydrophobic BM surface outperformed the hydrophilic MIL surface in the amount of water collected at the respective inclination angles (30, 45, and 60°). This is possibly attributed to the orientation angle of the functional surface toward the direction of moisture generation, and it shows that a 60° inclination angle is a good orientation angle to be utilized in harvesting atmospheric water.

https://doi.org/10.1021/acsomega.2c04344
ACS Omega 2022, 7, 43574−43581

4. CONCLUSIONS

In conclusion, a novel hydrophobic surface was fabricated and designed with the PDMS substrate and ($CaCl_2$) nanoparticles. From the experimental data, it is obvious that inclination angles through the force of gravity play a crucial role in efficient water collection. The presence of the microgroove textures helps absorbed tiny droplets on the MIL surface. Unlike the BM surface where large droplets sit on the microgroove pillars while tiny droplets trap in-between the pillars before finally running off to be collected. Such a surface allows droplets to be removed rapidly with a fast runoff time compared to the MIL surface. Here, we have demonstrated that the state-of-the-art hydrophobic BM surface outperforms the natural hydrophilic MIL surface in atmospheric water harvesting at the respective orientation angles 30, 45, and 60°. It is noteworthy to mention that the BM surface has a good efficient water collection rate at an inclination angle of 60° over other orientation angles and the MIL surface. The hydrophobic BM surface having higher contact angle hysteresis, transports water most rapidly to be harvested with a comparative advantage over the MIL surface. The advantage of the BM surface in water collection increases at a higher angle of inclination over the MIL surface. With 60° inclination, gravitational force tendency is increased, which means that gravity overcomes droplet pinning and retention forces on both surfaces. Overall, our results indicate that the designed surface greatly influences water collection, especially in arid regions without compromising droplet mobility. Finally, this result provides an insight into the design of a surface with a well-defined angle of inclination good enough for efficient and fast water collection.

AUTHOR INFORMATION

Corresponding Author

Edward Hingha Foday, Jr − *Department of Environmental Engineering, School of Water and Environment, Chang'an University, Xi'an, Shaanxi Province 710064, P.R China; Faculty of Education, Eastern Technical University of Sierra Leone, Kenema City 00232, Sierra Leone;* orcid.org/0000-0001-8687-2173; Email: hinghaja@gmail.com

Authors

Taiwo Sesay − *School of Highway, Chang'an University, Xi'an, Shaanxi Province 710064, P.R China*

Yagbasuah Maada Baion − *College of Economics and Management, Jilin Agricultural University, Changchun 130118, China*

Emmanuel Bartholomew Koroma − *Department of Geography-Environment and Natural Resources Management, Faculty of Social and Management Sciences, Ernest Bai Koroma University of Science and Technology, Magburaka City 00232, Sierra Leone*

Alpha Yayah Jalloh − *School of Economics and Management, Chang'an University, Xi'an 710064, China*

Kejan Kokofele − *Faculty of Education, Eastern Technical University of Sierra Leone, Kenema City 00232, Sierra Leone*

Florence Wuyah Baion − *Faculty of Education, Eastern Technical University of Sierra Leone, Kenema City 00232, Sierra Leone*

Complete contact information is available at: https://pubs.acs.org/10.1021/acsomega.2c04344

Notes

The authors declare no competing financial interest.

ACKNOWLEDGMENTS

The authors would like to acknowledge the Key Laboratory of Subsurface Hydrology and Ecological Effects in Arid Region of the Ministry of Education, Chang'an University, Xi'an 710064, Shaanxi, China, for providing us with the enabling environment to do our experiment.

REFERENCES

(1) Officer, P., *Food and agriculture organization of the United Nations*; FAO: Italy 2016.

(2) Supply, W. U. J. W.; Programme, S. M., *Progress on sanitation and drinking water: 2015 update and MDG assessment*; World Health Organization: 2015.

(3) Oki, T.; Kanae, S. Global hydrological cycles and world water resources. *Science* **2006**, *313*, 1068−1072.

(4) Foday, E. H., Jr.; Ramli, N. A. s.; Ismail, H. N.; Malik, N. A.; Basri, H. F.; Aziz, F. S. A.; Nor, N. S. M.; Jumhat, F. Municipal solid waste characteristics in Taman Universiti, Skudai, Johore, Malaysia. *J. Adv. Res.* **2017**, *38*, 13−20.

(5) Schiermeier, Q. Water risk as world warms. *Nature* **2014**, *505*, 10.

(6) Sharma, V.; Yiannacou, K.; Karjalainen, M.; Lahtonen, K.; Valden, M.; Sariola, V. Large-scale efficient water harvesting using bioinspired micro-patterned copper oxide nanoneedle surfaces and guided droplet transport. *Nanoscale Adv.* **2019**, *1*, 4025−4040.

(7) Foday, E. H., Jr.; Bo, B.; Xu, X. Removal of toxic heavy metals from contaminated aqueous solutions using seaweeds: A review. *Sustainability* **2021**, *13*, 12311.

(8) Clarke, R., *Water: the international crisis*; Routledge: 2013.

(9) Feron, S.; Cordero, R. R.; Damiani, A.; Jackson, R. B. Climate change extremes and photovoltaic power output. *Nat. Sustain.* **2021**, *4*, 270−276.

(10) Fuso Nerini, F.; Sovacool, B.; Hughes, N.; Cozzi, L.; Cosgrave, E.; Howells, M.; Tavoni, M.; Tomei, J.; Zerriffi, H.; Milligan, B. Connecting climate action with other Sustainable Development Goals. *Nat. Sustain.* **2019**, *2*, 674−680.

(11) Yao, J.; Yang, G. An efficient solar-enabled 2D layered alloy material evaporator for seawater desalination. *J. Mater. Chem. A* **2018**, *6*, 3869−3876.

(12) Klemm, O.; Schemenauer, R. S.; Lummerich, A.; Cereceda, P.; Marzol, V.; Corell, D.; Van Heerden, J.; Reinhard, D.; Gherezghiher, T.; Olivier, J.; et al. Fog as a fresh-water resource: overview and perspectives. *Ambio* **2012**, *41*, 221−234.

(13) Shan, H.; Pan, Q.; Xiang, C.; Poredoš, P.; Ma, Q.; Ye, Z.; Hou, G.; Wang, R. High-yield solar-driven atmospheric water harvesting with ultra-high salt content composites encapsulated in porous membrane. *Cell Rep. Phys. Sci.* **2021**, *2*, No. 100664.

(14) Tu, Y.; Wang, R.; Zhang, Y.; Wang, J. Progress and expectation of atmospheric water harvesting. *Joule* **2018**, *2*, 1452−1475.

(15) Zhang, L.; Wu, J.; Hedhili, M. N.; Yang, X.; Wang, P. Inkjet printing for direct micropatterning of a superhydrophobic surface: toward biomimetic fog harvesting surfaces. *J. Mater. Chem. A* **2015**, *3*, 2844−2852.

(16) Bhushan, B., Bioinspired Strategies for Water Collection and Water Purification. In *Biomimetics*; Springer: 2018; pp. 665−701.

(17) Ejeian, M.; Wang, R. Z. Adsorption-based atmospheric water harvesting. *Joule* **2021**, *5*, 1678−1703.

(18) Yang, K.; Pan, T.; Lei, Q.; Dong, X.; Cheng, Q.; Han, Y. A roadmap to sorption-based atmospheric water harvesting: from molecular sorption mechanism to sorbent design and system optimization. *Environ. Sci. Technol.* **2021**, *55*, 6542−6560.

(19) Zhang, Y.; Guo, S.; Yu, Z. G.; Qu, H.; Sun, W.; Yang, J.; Suresh, L.; Zhang, X.; Koh, J. J.; Tan, S. C. An Asymmetric Hygroscopic Structure for Moisture-Driven Hygro-Ionic Electricity Generation and Storage. *Adv. Mater.* **2022**, No. 2201228.

(20) Parker, A. R.; Lawrence, C. R. Water capture by a desert beetle. *Nature* **2001**, *414*, 33−34.
(21) Andrews, H. G.; Eccles, E. A.; Schofield, W. C. E.; Badyal, J. P. S. Three-dimensional hierarchical structures for fog harvesting. *Langmuir* **2011**, *27*, 3798−3802.
(22) Santos, M. J.; White, J. A. Theory and simulation of angular hysteresis on planar surfaces. *Langmuir* **2011**, *27*, 14868−14875.
(23) Zhu, H.; Guo, Z.; Liu, W. Biomimetic water-collecting materials inspired by nature. *Chem. Commun.* **2016**, *52*, 3863−3879.
(24) Liu, X.; Liang, Y.; Zhou, F.; Liu, W. Extreme wettability and tunable adhesion: biomimicking beyond nature? *Soft Matter* **2012**, *8*, 2070−2086.
(25) Lee, A.; Moon, M.-W.; Lim, H.; Kim, W.-D.; Kim, H.-Y. Water harvest via dewing. *Langmuir* **2012**, *28*, 10183−10191.
(26) Wang, Y.; Wang, X.; Lai, C.; Hu, H.; Kong, Y.; Fei, B.; Xin, J. H. Biomimetic water-collecting fabric with light-induced super-hydrophilic bumps. *ACS Appl. Mater. Interfaces* **2016**, *8*, 2950−2960.
(27) Sun, J.; Bhushan, B. Structure and mechanical properties of beetle wings: a review. *RSC Adv.* **2012**, *2*, 12606−12623.
(28) Zhai, L.; Berg, M. C.; Cebeci, F. Ç.; Kim, Y.; Milwid, J. M.; Rubner, M. F.; Cohen, R. E. Patterned superhydrophobic surfaces: toward a synthetic mimic of the Namib Desert beetle. *Nano Lett.* **2006**, *6*, 1213−1217.
(29) Garrod, R. P.; Harris, L. G.; Schofield, W. C. E.; McGettrick, J.; Ward, L.; Teare, D. O. H.; Badyal, J. P. S. Mimicking a Stenocara Beetle's back for microcondensation using plasmachemical patterned superhydrophobic− superhydrophilic surfaces. *Langmuir* **2007**, *23*, 689−693.
(30) Zhu, H.; Guo, Z. Hybrid engineered materials with high water-collecting efficiency inspired by Namib Desert beetles. *Chem. Commun.* **2016**, *52*, 6809−6812.
(31) White, B.; Sarkar, A.; Kietzig, A.-M. Fog-harvesting inspired by the Stenocara beetle—An analysis of drop collection and removal from biomimetic samples with wetting contrast. *Appl. Surf. Sci.* **2013**, *284*, 826−836.
(32) Prakash, M.; Quéré, D.; Bush, J. W. M. Surface tension transport of prey by feeding shorebirds: the capillary ratchet. *Science* **2008**, *320*, 931−934.
(33) Chen, H.; Zhang, P.; Zhang, L.; Liu, H.; Jiang, Y.; Zhang, D.; Han, Z.; Jiang, L. Continuous directional water transport on the peristome surface of Nepenthes alata. *Nature* **2016**, *532*, 85−89.
(34) Al-Sharafi, A.; Yilbas, B. S.; Sahin, A. Z.; Ali, H.; Al-Qahtani, H. Heat transfer characteristics and internal fluidity of a sessile droplet on hydrophilic and hydrophobic surfaces. *Appl. Therm. Eng.* **2016**, *108*, 628−640.
(35) Tuck, E. O.; Schwartz, L. W. Thin static drops with a free attachment boundary. *J. Fluid Mech.* **1991**, *223*, 313−324.
(36) Annapragada, S. R.; Murthy, J. Y.; Garimella, S. V. Prediction of droplet dynamics on an incline. *Int. J. Heat Mass Transfer* **2012**, *55*, 1466−1474.
(37) Thampi, S. P.; Adhikari, R.; Govindarajan, R. Do liquid drops roll or slide on inclined surfaces? *Langmuir* **2013**, *29*, 3339−3346.
(38) Aussillous, P.; Quéré, D. Shapes of rolling liquid drops. *J. Fluid Mech.* **2004**, *512*, 133−151.
(39) Yilbas, B. S.; Al-Sharafi, A.; Ali, H.; Al-Aqeeli, N. Dynamics of a water droplet on a hydrophobic inclined surface: influence of droplet size and surface inclination angle on droplet rolling. *RSC Adv.* **2017**, *7*, 48806−48818.
(40) Young, T. III. An essay on the cohesion of fluids. *Philos. Trans. R. Soc. London* **1805**, *95*, 65−87.
(41) Foday, E. H., Jr.; Bai, B. Mangifera indicaLeaf (MIL) as a Novel Material in Atmospheric Water Collection. *ACS Omega* **2022**, *7*, 11809−11817.
(42) Muth, C. M.; Shank, E. S. Gas embolism. *N. Engl. J. Med.* **2000**, *342*, 476−482.
(43) Tang, Z.; Li, Y.; Zhang, B.; Wang, M.; Li, Y. Controlling rice leaf breaking force by temperature and moisture content to reduce breakage. *Agronomy* **2020**, *10*, 628.

https://doi.org/10.1021/acsomega.2c04344
ACS Omega 2022, 7, 43574−43581